American Journal of Preventive Cardiology 31 (2027) 101732

Contents lists available at ScienceDirect

American Journal of Preventive Cardiology

journal homepage: www.journals.elsevier.com/american-journal-of-preventive-cardiology

Heart failure and atrial fibrillation prediction from non-gated chest CT scans using AI-based cardiac chamber volumetry: an AI-CVD study within the multi-ethnic study of atherosclerosis (MESA)

Seyed Reza Mirjalili [a], Kyle Atlas [a], Anthony P. Reeves [b], Chenyu Zhang [a], Jakob Wasserthal [c], Amir Azimi [a], Ali Hashemi [a], Mohammadhossein Mozafarybazargany [a], Amir Ghaffari Jolfayi [a], Thomas Atlas [d], Claudia I. Henschke [e], David F. Yankelevitz [e], Javier J. Zulueta [e], Wenjun Fan [f], Jeffrey I. Mechanick [g], Andrea D. Branch [e], Khurram Nasir [h], Zahi Fayad [i], Michael V. McConnell [j], Jamal S. Rana [k], Rozemarijn Vliegenthart [l], David J. Maron [j], Jagat Narula [m], Matthew J. Budoff [n], Roxana Mehran [e], Kim A. Williams Sr [o], Prediman K. Shah [p], Oren Mechanic [q], Arthur S Agatston [q], Robert A. Kloner [r], Nathan D. Wong [s], Morteza Naghavi [a,*]

[a] HeartLung.AI, Houston, TX, 77021, USA
[b] Department of Electrical and Computer Engineering, Cornell University, Ithaca, NY. 14853, USA
[c] Clinic of Radiology and Nuclear Medicine, University Hospital Basel, Petersgraben 4, CH-4031 Basel, Switzerland
[d] Tustin Teleradiology, Tustin, CA 92780, USA
[e] Icahn School of Medicine at Mount Sinai, New York, NY 10029, USA
[f] Department of Epidemiology and Biostatistics, Wen School of Public Health, University of California, Irvine, USA
[g] Kravis Center for Clinical Cardiovascular Health, Mount Sinai Fuster Heart Hospital, New York, NY 10029 USA
[h] Houston Methodist Hospital, Houston, TX 77030, USA
[i] BioMedical Engineering and Imaging Institute. Icahn School of Medicine at Mount Sinai, New York, NY 10029, USA
[j] Stanford Prevention Research Center, Stanford University School of Medicine, Stanford, CA, 94305, USA
[k] Division of Cardiology, Kaiser Permanente Oakland Medical Center, California, USA
[l] Department of Radiology, University Medical Center Groningen, GZ 9713, Netherlands
[m] University of Houston, Houston, TX, 77030, USA
[n] The Lundquist Institute, CA 90502, USA
[o] University of Louisville, Louisville, KY, 40202, USA
[p] Cedars-Sinai Medical Center, Los Angeles, CA 90048, USA
[q] The Agatston Center, Miami Beach, Florida, USA
[r] Huntington Medical Research Institutes, Pasadena, CA, 91105, USA and Keck School of Medicine of University of Southern California, Los Angeles, CA 90033, USA
[s] Heart Disease Prevention Program, Mary and Steve Wen Cardiovascular Division, University of California Irvine School of Medicine, CA 92697, USA

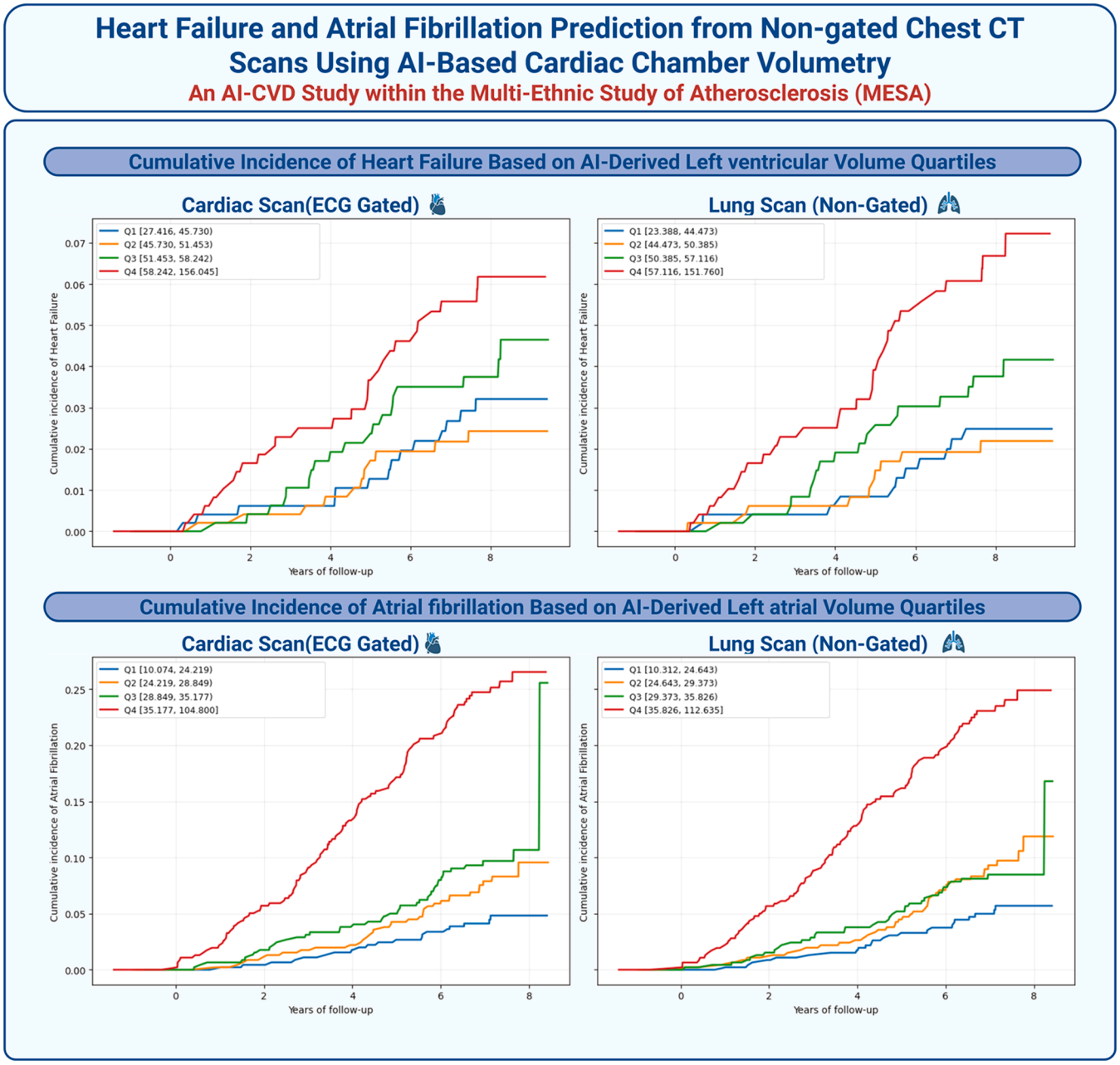
* Corresponding author at: HeartLung.AI, Houston, TX, 77021, USA.
E-mail address: mn@vp.org (M. Naghavi).

https://doi.org/10.1016/j.ajpc.2026.101732

Available online 5 July 2026
2666-6677/© 2026 The Authors. Published by Elsevier B.V. This is an open access article under the CC BY-NC-ND license (http://creativecommons.org/licenses/by-nc-nd/4.0/).

G R A P H I C A L A B S T R A C T

Central illustration.



A R T I C L E I N F O

Keywords:
Computed tomography
Artificial intelligence
Atrium
Ventricle
Cardiovascular disease

A B S T R A C T

Background: We previously demonstrated that AI-derived cardiac chamber volumetry in ECG-gated CT scans predicts atrial fibrillation (AF) and heart failure (HF). Since most chest CTs are non-gated, and the American Heart Association recently highlighted their value for opportunistic cardiovascular risk assessment using AI-based coronary artery calcium scoring, we extended this concept to evaluate whether AI-derived chamber volumetry from non-gated CTs can reliably predict HF and AF.s

Methods: We compared AI-derived chamber volumetry from non-gated and ECG-gated chest CTs in 2053 Multi-Ethnic Study of Atherosclerosis (MESA) Exam 5 participants using mean and standard-deviation of absolute differences, intraclass correlation coefficients (ICC), and Cohen's κ. Variability between paired ECG-gated scans was determined by analyzing scans acquired 2 min apart in 5749 MESA Exam 1 participants. Predictive performance for incident HF and AF was compared using cumulative incidence curves, age- and sex-adjusted C-indices, and non-inferiority testing (δ=0.05).

Results: Non-gated scans demonstrated excellent overall agreement with ECG-gated scans, with comparable performance for detecting cardiac chamber enlargement (98.8–99.2%, κ=0.76–0.84), relative to agreement observed between paired ECG-gated scans (98.6–98.9%, κ=0.72–0.77). Cumulative incidence curves for HF and AF stratified by quartiles showed substantial overlap. Age- and sex-adjusted C-indices were comparable for left atrial volume (0.75 vs 0.74, $p = 0.001$, non-inferiority $p < 0.001$), ventricular volume (both 0.77, $p = 0.97$, non-inferiority $p < 0.001$), and ventricular ratio (both 0.74, $p = 0.57$, non-inferiority $p < 0.001$) in predicting AF and HF.

Conclusion: AI-based evaluation of non-gated chest CT may provide reliable cardiac chamber volumetry and cardiovascular outcome prediction, enabling opportunistic screening for HF and AF risk.

1. Introduction

Approximately 20 million chest computed tomography (CT) examinations are performed annually in the United States for various clinical indications, [1] including the evaluation of chronic obstructive pulmonary disease (COPD) [2], lung cancer screening [3], assessment of chest trauma[4], and the diagnosis and evaluation of chest infections [5] and interstitial lung disease [6]. The majority of these scans are non-gated (NCCT) studies. ECG-gated acquisitions account for <5% of all chest CT examinations [7]. Beyond their intended clinical use and regardless of the primary indication for imaging, artificial intelligence (AI) can opportunistically extract a wide range of additional information from NCCT scans efficiently and with high reliability [8].

The AI-CVD initiative was established to extract clinically meaningful information beyond the conventional Agatston score from ECG-gated NCCT scans [8]. Among the metrics opportunistically derived using AI, cardiac chamber volumes are particularly valuable, previously shown to be comparable to cardiac MRI measurements [9], with AI-derived left atrial (LA) volume predicting atrial fibrillation (AF) [10], and left ventricular volume (LV), mass (LVM), and left-to-right ventricular volume ratio (LV/RV) predicting heart failure (HF)[11,12]. Notably, these findings were derived exclusively from ECG-gated NCCT. More recently, however, the American Heart Association (AHA) has highlighted the potential of non-gated NCCT scans to transform clinical practice by enhancing cardiovascular risk prediction and enabling broader, more equitable population coverage through opportunistic AI applications [13].

In ECG-gated scans, image acquisition is synchronized with the mid-diastolic phase of the cardiac cycle, when cardiac motion is minimal, thereby reducing motion artifacts caused by the heartbeat [14]. This timing is critical because cardiac chamber volumes vary throughout systole and diastole. Conversely, in non-gated chest CT scans, the specific phase of the cardiac cycle during which the image is captured varies [15], potentially influencing the predictive performance of chamber volume measurements for cardiovascular outcomes.

Therefore, the objectives of this study were threefold. First, we aimed to evaluate the differences between AI-derived cardiac chamber measurements obtained from non-gated and ECG-gated NCCT scans acquired from the same individuals on the same day. Second, we sought to determine whether these differences were comparable to the variation observed between two paired ECG-gated NCCT scans acquired within a two-minute interval. Third, we compared the predictive performance of AI-derived cardiac chamber measurements from non-gated versus ECG-gated NCCT scans for incident HF and AF.

2. Methods

2.1. Study population

The Multi-Ethnic Study of Atherosclerosis (MESA) is a large, multicenter, prospective cohort study conducted across six sites in the United States: Baltimore (Maryland), Los Angeles (California), Chicago (Illinois), Forsyth County (North Carolina), New York City (New York), and St. Paul (Minnesota). The study was designed to enroll individuals free of clinically apparent cardiovascular disease (CVD) at Exam 1. Participants were excluded if they had a known history of cardiovascular disease, a physician diagnosis of angina, or any prior invasive cardiac procedures, including coronary artery bypass grafting, percutaneous coronary intervention, valve surgery, pacemaker implantation, or vascular surgery. Each examination included comprehensive data collection encompassing detailed medical history, physical examination, laboratory testing, and CT imaging. More detailed information about MESA cohort is publicly available at https://mesa-nhlbi.org/.

This study utilized data from examinations 1 and 5 of the MESA. In MESA Exam 1 (2000–2002), each participant underwent two paired ECG-gated NCCT scans obtained with a 2-minute breathing rest between scanning. The positioning of the participants remained the same for both series [16]. In MESA Exam 5 (2010–2012), both ECG-gated and non-gated NCCT scans, were acquired from participants on the same day [17,18]. Based on the exclusion criteria of the MESA study, a total of 6814 participants were initially enrolled in MESA Exam 1 and underwent paired ECG-gated CT scans [19]. In MESA Exam five, 4655 participants were enrolled [20], among whom 2607 had both ECG-gated and non-gated CT scans available [21]. For first exam, 771 participants, and for exam five, 163 participants, did not provide consent for the use of their CT scans for commercial purposes. Detailed information about CT scan protocols and outcome definitions is available in the **Supplementary Materials**.

For the comparison of cardiovascular outcome predictive performance between non-gated and ECG-gated CT scans, data from MESA Exam 5 were used as the baseline for this analysis, as this was the only examination that included both scan types. Participants included in this analysis were followed for incident HF over a median of 8.1 years and for incident AF over a median of 7.1 years.

This study was carried out in accordance with the ethical standards set forth in the Declaration of Helsinki. The MESA protocol was approved by the Institutional Review Boards of all six participating centers and by the National Heart, Lung, and Blood Institute. All participants provided written informed consent before enrollment.

2.2. AI-enabled chamber volumetry using non-contrast chest CT scans

Cardiac chamber volumes were quantified using an FDA-approved, AI-based automated volumetry software (FDA registration K240786), AutoChamber Version 2.0 (HeartLung.AI, Houston, TX), which operates as part of the AI-CVD platform. The AI-CVD system is an advanced AI framework designed to opportunistically analyze existing CT scans to identify subclinical markers of multiple conditions, including CVD, osteoporosis, and COPD. Further information on the development, validation, performance, previous publications, and work process of the AI-CVD and AutoChamber tools is provided in the **Supplementary Materials**.

For each cardiac chamber, the quality of the NCCT images was evaluated based on whether the target chamber was fully contained within the field of view and did not touch any of its boundaries, to ensure suitability for analysis using AutoChamber. The proportion of participants who passed the quality check for each cardiac chamber is reported in detail in the **Table S1**. Pairs of NCCT scans targeted for

comparison were included in the analysis only if both scans passed the quality assessment.

2.3. Statistical analysis

All statistical analyses were performed using Python version 3.11. Continuous variables were described as mean ± standard deviation (SD) or median with interquartile range. Categorical variables were reported as percentages. Differences between participants who developed HF or AF during follow-up and those who did not, were evaluated using independent *t*-tests or Mann–Whitney U tests for continuous variables, as appropriate. Chi-square tests were applied to compare categorical variables. All statistical tests were two-sided, and a p-value < 0.05 was considered statistically significant.

We evaluated the presence of enlarged cardiac chambers on ECG-gated scans (defined as values ≥97.5th percentile of ECG-gated measurements) and on non-gated scans (defined as values ≥97.5th percentile of non-gated measurements) [22,23]. The chance-corrected agreement between the two scan types for detecting enlarged chambers was assessed using Cohen's Kappa statistic (κ) and visualized with a Venn diagram. To assess the reproducibility of AI-derived chamber volumetry, we applied the Bland–Altman method [24]. The absolute differences between non-gated and ECG-gated NCCT, as well as between paired ECG-gated scans, were calculated for each cardiac chamber. This difference was referred to as the absolute rescan difference, with the limits of agreement (LoA) defined as ±1.96 SD of the absolute difference. The variability of the absolute rescan difference was quantified using the SD. Additionally, intraclass correlation coefficients (ICC) were computed to evaluate the consistency of chamber volume measurements across acquisition types. These reproducibility metrics determined whether the variability observed between non-gated and gated scans was comparable to the expected variation between two ECG-gated measurements in the same individual.

To compare predictive performance of non-gated and ECG-gated NCCT, AI-derived cardiac chamber measurements, including those of the LA, LV, and LV mass, were indexed to body surface area (BSA) to account for body size differences. The resulting parameters included the left atrial volume index (LAVI), left ventricular volume index (LVVI), and left ventricular mass index (LVMI). The LV/RV ratio was defined as the LV volume divided by the right ventricular (RV) volume. Specifically, we evaluated the cumulative incidence of cardiovascular outcomes across quartiles of LAVI for AF, and across quartiles of LVVI, LVMI and LV/RV ratio for HF. In addition, we performed a non-inferiority analysis comparing discriminative performance of non-gated and ECG-gated NCCT parameters using Harrell's concordance index (C-index). Separate Cox proportional hazards models were fitted for each acquisition type. Models were adjusted for age and sex. The difference in C-index (non-gated minus ECG-gated) was estimated with 95% confidence intervals derived from 2000 paired bootstrap resamples using the percentile method. Non-inferiority was pre-specified with a margin of -0.05, meaning non-gated measurements would be considered non-inferior if the lower bound of the 95% confidence interval for the C-index difference did not exceed - 0.05. This margin was chosen as it represents the smallest clinically meaningful difference in discriminative ability. A one-sided p-value for non-inferiority was calculated as the proportion of bootstrap samples where the difference exceeded the non-inferiority margin. Additionally, a two-sided test was performed to evaluate whether the difference in C-index between modalities was statistically significant, with the p-value computed from the bootstrap distribution. In supplementary analyses, we performed Cox proportional hazards regression reporting hazard ratios (HR) per one SD increase in each chamber volume index for all outcomes, using both ECG-gated and non-gated measurements. Additionally, we extended our primary analytic framework, to HF subtypes (HF with preserved ejection fraction [HFpEF] and HF with reduced ejection fraction HFrEF) and all-cause mortality.

3. Results

A total of 2053 participants from MESA Exam 5 were included in the analysis. Among them, 46 had prevalent HF and 146 had prevalent AF at the time of exam 5, while 72 participants developed HF and 208 developed AF during follow-up. Table 1 presents the population characteristics at Exam 5 and compares participants who developed incident HF or AF during follow-up with those who did not.

3.1. Non-gated vs. ECG-Gated CT scans

The mean volume of LA was 61.19 mL in non-gated scans and 59.74 mL in ECG-gated scans and (difference, 1.45 mL). The SD of the absolute rescan difference was 7.23 mL (Table 2), and the LoA ranged from −12.73 to 15.63 mL (Fig. 1). Median and interquartile range of differences is visible in **Figure S1**. ICC was 0.94, indicating excellent agreement between non-gated and gated scans. The overall agreement for detecting enlarged (≥ 97.5th percentile) LA between the two scan types was 99.1%, with only a small number of discordant cases (18 of 1994 participants), in which enlargement was identified on one scan type but not the other. Furthermore, the chance-corrected agreement, represented by the κ statistic, was high ($\kappa = 0.81$) (Fig. 2).

The mean LV volume was 99.97 mL in non-gated scans and 102.11 mL in ECG-gated scans (difference, −2.14 mL). The SD of the paired differences was 7.76 mL (Table 2), and the limits of agreement ranged from −17.35 to 13.06 mL (Fig. 1). The ICC was 0.95, indicating excellent agreement between scan types. The overall agreement for detecting LV enlargement was 99.2%, with few discordant cases (16 of 2010 participants). The chance-corrected agreement was also high ($\kappa = 0.84$) (Fig. 2).

The mean LVM was 104.32 g in non-gated scans and 106.90 g in ECG-gated scans (difference, −2.59 g). The SD of the paired differences was 10.64 g (Table 2), and the limits of agreement ranged from −23.44 to 18.26 g (Fig. 1). The ICC was 0.96, indicating excellent agreement between scan types. The overall agreement for detecting LVM enlargement was 98.9%, with a small number of discordant cases (22 of 1980 participants). The κ statistic indicated substantial agreement ($\kappa = 0.77$) (Fig. 2).

The mean LV/RV ratio was 0.84 in non-gated scans and 0.82 in ECG-gated scans (difference, 0.02). The SD of the paired differences was 0.05 (Table 2), and the limits of agreement ranged from −0.08 to 0.11 (Fig. 1). The ICC was 0.89, indicating good agreement between scan types. The overall agreement for identifying elevated LV/RV ratio was 98.8%, with few discordant cases (22 of 1858 participants). The κ statistic indicated substantial agreement ($\kappa = 0.76$) (Fig. 2).

3.2. Comparing paired ECG-gated CT scans

When comparing two paired ECG-gated scans, all chamber measurements and the LV/RV ratio demonstrated lower mean absolute rescan differences, reduced variability of the absolute rescan difference, and improved ICCs (Table 2) compared with comparison of the non-gated and ECG-gated scans. Overall agreement for identifying enlarged chambers between the two ECG-gated scans was comparable to that observed in the non-gated versus ECG-gated comparison (Fig. 2). A detailed comparison between the two paired ECG-gated scan results is provided in the **Supplementary Materials**.

3.3. Non-gated vs. ECG-Gated CT scans in predicting outcomes

Cumulative incidence curves for HF stratified by quartiles showed substantial overlap between non-gated and ECG-gated scans (Fig. 3). Participants in the highest quartile of LVVI based on non-gated scans had a HF incidence of 8.5 per 1000 person-years, compared with 7.6 in the highest quartile of ECG-gated scans. Corresponding values for the LV/RV ratio were 7.6 and 7.9, respectively and 9.7 and 9.6 for LVMI.

Table 1
Baseline (MESA Exam Five) clinical characteristics of participants according to heart failure and atrial fibrillation incidence.

Variables	Total Population	Heart Failure Follow-up			Atrial Fibrillation Follow-up		
	(N = 2053)	No Incidence (N = 1932)	Incident (N = 72)	p-value	No Incidence (N = 1696)	Incident (N = 208)	p-value
Age (Years)	70.0 ± 9.3	69.9 ± 9.3	76.7 ± 8.9	< 0.001	69.0 ± 9.1	74.7 ± 8.5	< 0.001
Sex (Male %)	47.6%	47.2%	52.8%	0.4	46.0%	57.2%	< 0.001
Race/Ethnicity							
White (%)	41.2%	41.1%	41.7%	1.0	40.0%	48.1%	< 0.001
Chinese (%)	10.6%	11.0%	5.6%	0.2	10.6%	9.1%	0.6
Black (%)	26.1%	25.9%	27.8%	0.8	26.9%	25.0%	0.6
Hispanic (%)	22.2%	22.0%	25.0%	0.6	22.5%	17.8%	0.1
Smoking							
Current smoker (%)	8.2%	8.3%	4.2%	0.3	8.9%	6.2%	0.3
Former smoker (%)	47.2%	46.4%	63.9%	< 0.001	46.4%	48.6%	0.6
Anthropometric Features							
Body mass index (Kg/m^2)	28.7 ± 5.6	28.6 ± 5.5	30.1 ± 5.7	0.0	28.7 ± 5.6	28.8 ± 5.4	0.7
Weight (Lb.)	173.6 ± 38.8	172.8 ± 38.3	184.8 ± 42.9	< 0.001	173.0 ± 38.7	179.1 ± 39.5	< 0.001
Height (cm)	165.4 ± 10.1	165.4 ± 10.0	166.5 ± 10.9	0.4	165.2 ± 9.9	167.5 ± 10.2	< 0.001
Waist circumference (cm)	99.8 ± 14.6	99.4 ± 14.5	106.2 ± 14.5	< 0.001	99.2 ± 14.5	103.0 ± 14.6	< 0.001
Hip circumference (cm)	105.8 ± 12.3	105.6 ± 12.2	108.4 ± 12.2	0.1	105.7 ± 12.4	106.7 ± 11.7	0.2
Lipid profile							
LDL-C (mg/dl)	104.7 ± 32.4	105.8 ± 32.1	87.6 ± 33.3	< 0.001	106.8 ± 32.2	95.0 ± 30.9	< 0.001
HDL-C (mg/dl)	55.2 ± 16.2	55.3 ± 16.2	54.0 ± 15.7	0.5	55.1 ± 16.0	55.6 ± 16.6	0.7
Total Cholesterol (mg/dl)	181.7 ± 37.1	182.8 ± 36.8	164.2 ± 39.3	< 0.001	183.9 ± 36.8	172.4 ± 35.2	< 0.001
Triglycerides (mg/dl)	96.0 [72.0–131.0]	96.0 [72.0–131.0]	94.0 [74.0–139.8]	0.8	96.0 [72.0–131.0]	98.0 [75.5–133.5]	0.4
Lipid medication consumption (%)	39.7	38.4	58.3	< 0.001	37.4%	50.5%	< 0.001
Glucose metabolism							
Diabetes mellitus (%)	42.7	41.7	61.1	< 0.001	41.3%	51.4%	< 0.001
Fasting blood glucose	102.5 ± 27.7	101.8 ± 26.4	109.1 ± 30.1	< 0.001	102.1 ± 26.6	104.5 ± 31.1	0.3
HbA1C	6.0 ± 0.9	5.9 ± 0.9	6.3 ± 1.0	< 0.001	6.0 ± 0.9	6.0 ± 0.9	0.2
Blood pressure							
SBP (mmHg)	124.2 ± 20.4	124.0 ± 20.5	130.4 ± 18.5	< 0.001	123.3 ± 20.2	128.2 ± 21.1	< 0.001
DBP (mmHg)	68.3 ± 10.0	68.5 ± 9.9	67.0 ± 10.2	0.2	68.4 ± 9.9	68.1 ± 10.5	0.7
HTN medication consumption (%)	56.2%	54.3%	83.3%	< 0.001	52.5%	71.2%	< 0.001
Coronary calcification							
Agatston score	41.0 [0.0–264.4]	33.9 [0.0–227.1]	260.4 [41.3–1074.7]	< 0.001	26.2 [0.0–194.9]	143.0 [16.5–529.2]	< 0.001

LDL-C: Low density lipoprotein cholesterol, HDL-C: High density lipoprotein cholesterol, HbA1c: Hemoglobin A1C, SBP: Systolic blood pressure, DBP: Diastolic blood pressure, HTN: Hypertension.

Table 2
Interscan reproducibility of AI-derived cardiac chamber volumetry based on CT gating status.

Chambers	Non-gated vs ECG-gated	ECG-gated a vs ECG-gated b
Rescan absolute differences		
Left atrial volume (cc)	1.45	0.57
Left ventricular volume (cc)	−2.14	0.45
Left ventricular mass (cc)	−2.59	0.56
Left-to-right ventricular ratio	0.02	0.002
Variability of rescan differences based on standard deviation		
Left atrial volume (cc)	7.23	5.22
Left ventricular volume (cc)	7.76	8.21
Left ventricular mass (cc)	10.64	6.88
Left-to-right ventricular ratio	0.05	0.04
Rescan inter covariate correlation		
Left atrial volume (cc)	0.94	0.95
Left ventricular volume (cc)	0.95	0.95
Left ventricular mass (cc)	0.96	0.96
Left-to-right ventricular ratio	0.89	0.92

Similarly, cumulative incidence curves for AF demonstrated close agreement between non-gated and ECG-gated scans, with the highest quartile of LAVI showing AF incidences per 1000 person-year of 36.5 and 39.2, respectively. A similarly substantial overlap in cumulative incidence curves was observed for all-cause mortality (**Figure S2**).

Across all HF predicting Cox models (LVVI, LVMI, and LV/RV), non-gated and ECG-gated CT demonstrated nearly identical discrimination, with minimal differences in C-index and no statistically significant differences (Table 3). In all cases, the lower bounds of the confidence intervals were well above the prespecified non-inferiority margin, confirming non-inferiority of the non-gated approach (all non-inferiority $p < 0.001$).

For AF, LAVI derived from ECG-gated scans showed slightly higher discrimination compared with non-gated scans, with a small but statistically significant difference. However, the magnitude of this difference remained within the prespecified non-inferiority margin, and non-gated LAVI was still considered non-inferior (Table 3). Similar findings were observed for the HFpEF, HFrEF and mortality outcomes (**Table S2)**. In addition, HR estimates per one SD increase were closely concordant between ECG-gated and non-gated measurements across all chamber volume indices and all outcomes (**Figure S3**)

4. Discussion

Our study provides the first, large-scale comparison of AI-derived cardiac chamber volumetry between non-gated chest CT and ECG-gated cardiac CT scans, addressing a major gap in the applicability of AI-based cardiac phenotyping across scan types. By leveraging >2000 paired scans from the MESA cohort, we demonstrate that chamber volumetry derived from non-gated CT, despite expected motion-related variability and differences across the cardiac cycle, can achieve predictive performance for HF and atrial AF comparable to that of ECG-gated scans. These findings highlight the potential of AI-based cardiac volumetry across heterogeneous imaging conditions and establish a foundation for opportunistic cardiac risk assessment using the large and growing repository of existing non-gated chest CT scans.

Previous studies have demonstrated that CAC scoring and epicardial fat quantification show comparable results between non-gated and ECG-

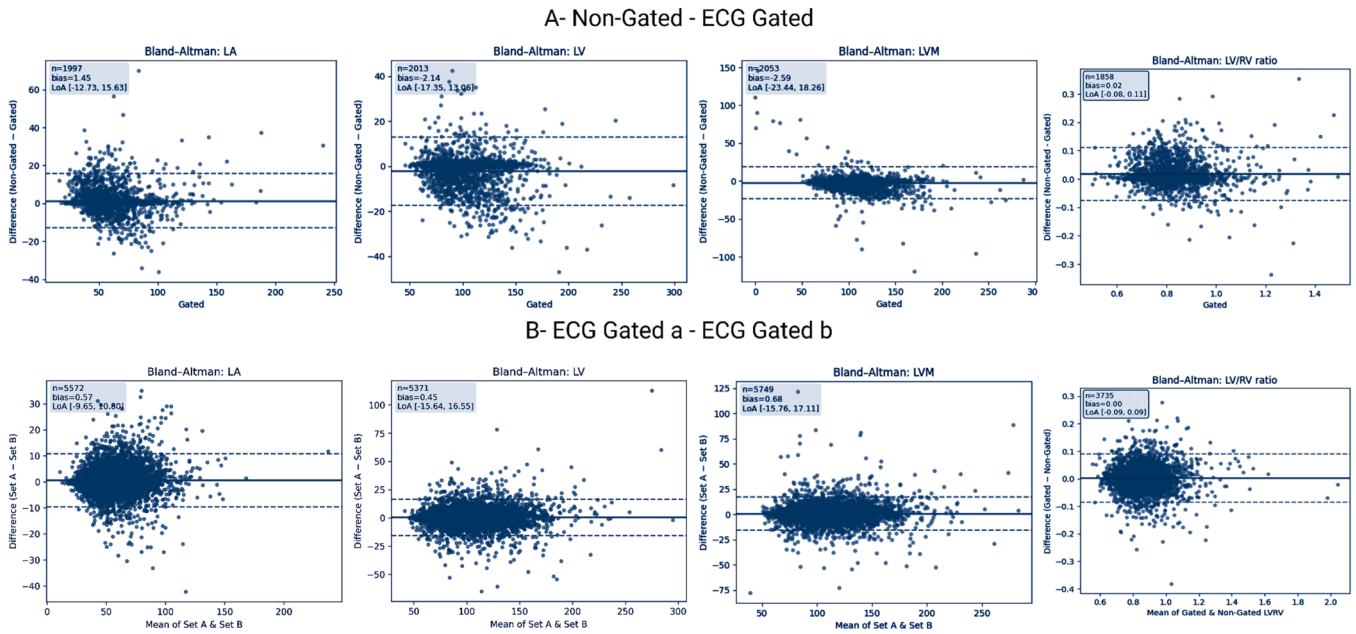


Fig. 1. Bland–Altman analysis comparing AI-derived cardiac chamber measurements between non-gated and ECG-gated CT scans, and paired ECG-gated scans. LA: Left atrium, LV: Left ventricle volume, LVM: Left ventricular mass, LV/RV: Left-to-right ventricular ratio, Bias: mean absolute rescan difference, LoA: Limits of agreement (±1.96 standard deviation).

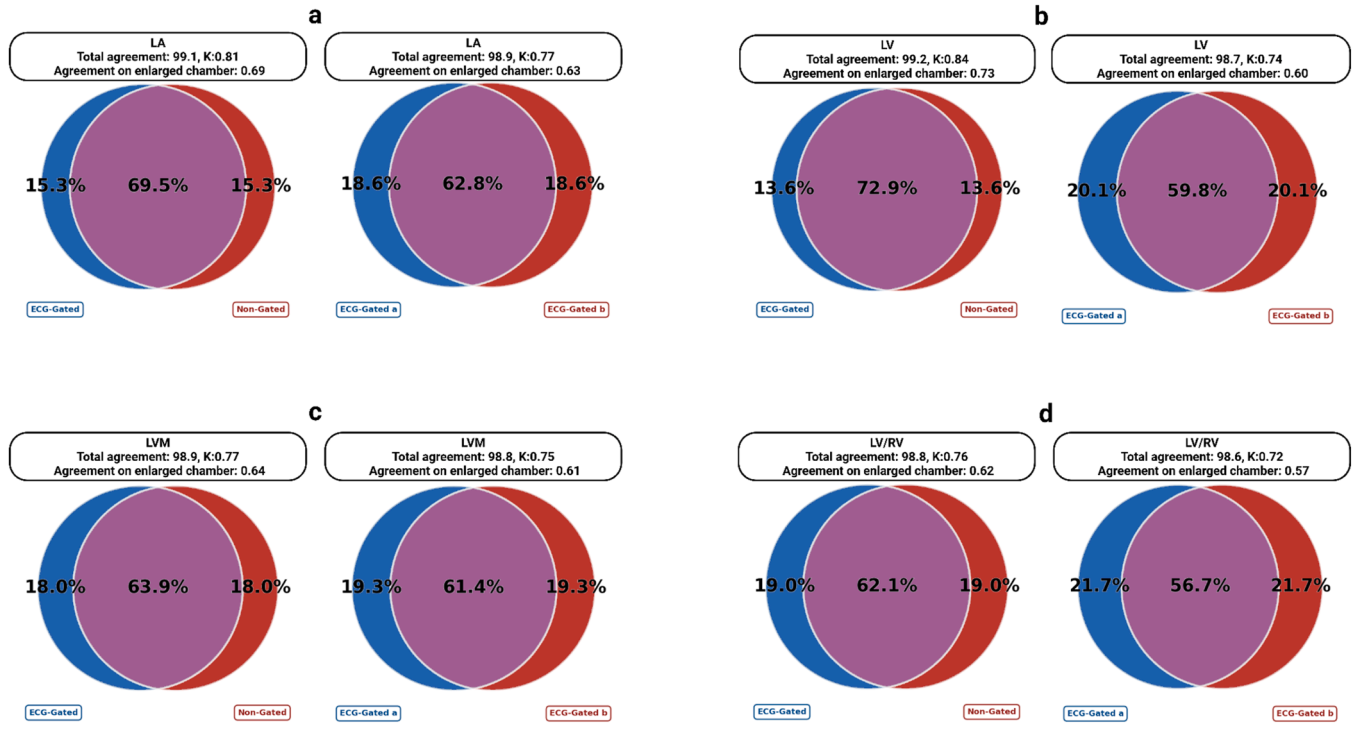


Fig. 2. Comparing agreement on chamber enlargement based on AI-derived cardiac chamber volumetry between non-gated and ECG-gated CT scans, and paired ECG-gated scans. a-Comparing agreement on left atrial volume enlargement, b- Comparing agreement on left ventricular volume enlargement, c- Comparing agreement on left ventricular mass enlargement, ᴅ- Comparing agreement on left-to-right ventricular ratio increase. LAVI: Left atrial volume index, LVVI: Left ventricular volume index, LVMI: Left ventricular mass index, LV/RV: Left-to-right ventricular ratio, κ: Cohen's Kappa statistic.

gated NCCT scans [25–29]. Moreover, a study comparing non-gated and ECG-gated contrast-enhanced CT scans in a small study of patients with pulmonary embolism reported a high degree of concordance between the two methods for cardiac ventricular measurements [30]. The scarcity of research on this topic can be attributed to the labor-intensive nature of manual or semi-automated segmentation methods [31], as well as the inherent limitations of NCCT imaging. The absence of intravenous contrast leads to poor differentiation between the blood pool and myocardium, making accurate segmentation and quantification of cardiac chambers particularly challenging [32]. However, the

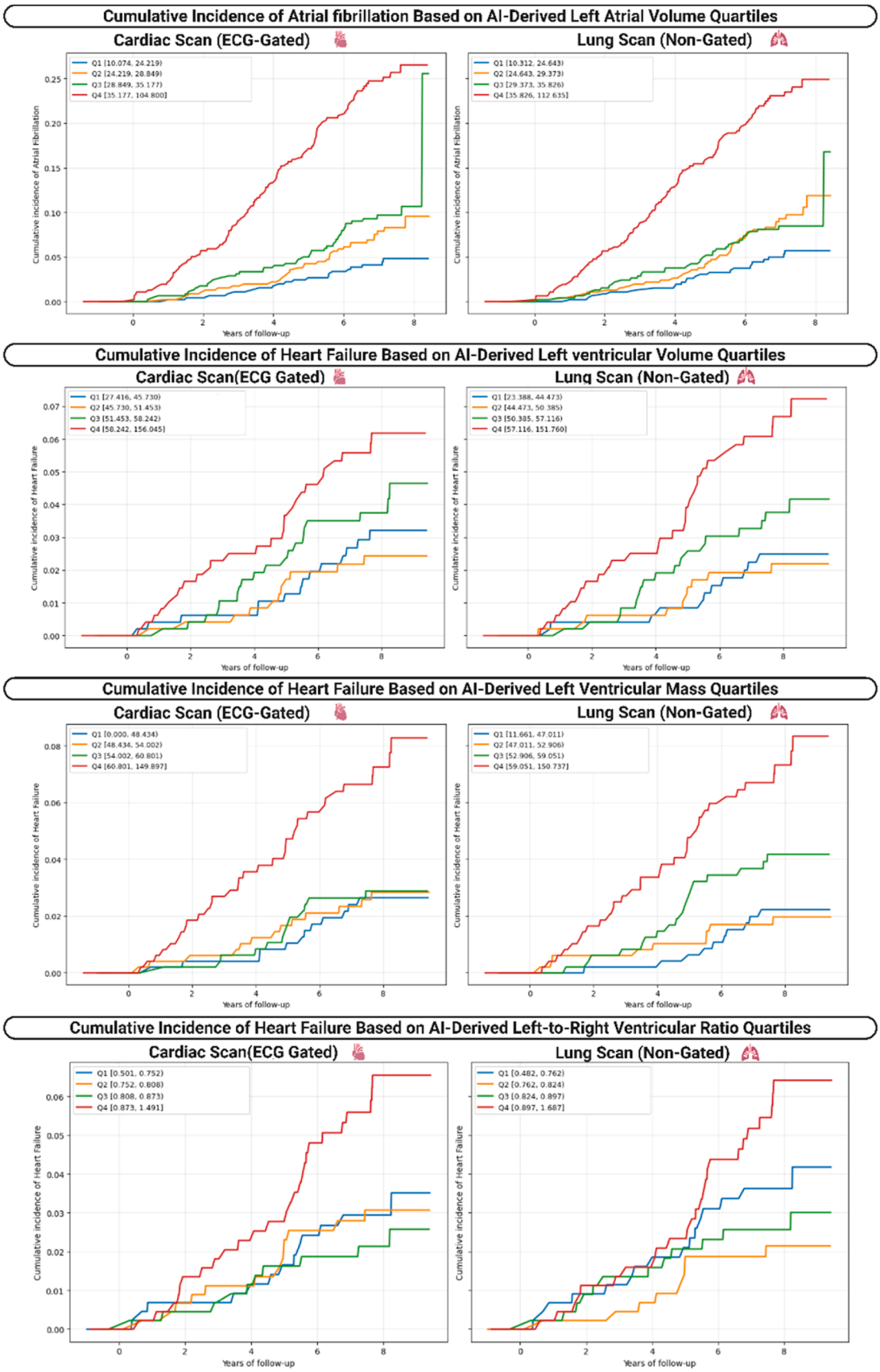


Fig. 3. Comparison of the cumulative incidence of heart failure and atrial fibrillation using AI-derived chamber volumetry from non-gated lung and ECG-gated cardiac CT.

Table 3
Comparative analysis of non-gated Lung and ECG-gated cardiac CT for AI-based prediction of atrial fibrillation and heart failure.

Chamber	ECG Gated C-Index	Non-Gated C-Index	Two-Sided p value	95% Confidence Interval of Difference	Lower bound of 95% CI of Difference	Pre-Specified δ Margin	Non-inferiority p value
	Heart Failure						
Left Ventricular Volume Index	0.772 (0.718–0.826)	0.771 (0.714–0.828)	0.97	(−0.018, 0.025)	−0.018	−0.05	< 0.001
Left Ventricular Mass Index	0.775(0.723 - 0.829)	0.774 (0.720–0.830)	0.95	(−0.018, 0.024)	−0.018	−0.05	< 0.001
Left-to-Right Ventricular Volume	0.743 (0.689- 0.801)	0.741(0.688- 0.800)	0.57	(−0.008, 0.011)	−0.008	−0.05	< 0.001
	Atrial Fibrillation						
Left Atrial Volume Index	0.752(0.720- 0.783)	0.737(0.706–0.771)	0.001	(−0.027–0.004)	- 0.027	−0.05	< 0.001

use of AI-based volumetry in our study overcame these limitations, enabling reliable chamber quantification and even demonstrating performance comparable to cardiac MRI in prior validations [9].

In ECG-gated CT, the goal is to capture images during mid-diastole, which typically corresponds to 50–80% of the R–R interval, depending on the heart rate [33]. In contrast, non-gated scans may capture images at any phase of the cardiac cycle. During mid-ventricular diastole, the ventricles are in the phase of passive filling, while the atria are in the conduit phase of emptying or diastasis just prior to atrial contraction. Consequently, images acquired during mid-diastole are expected to demonstrate larger ventricular volumes and comparable or smaller atrial volumes compared with those obtained during other phases of the cardiac cycle [34]. This physiological expectation is consistent with our findings, which demonstrated a negative absolute rescan difference (Non-gated – ECG-gated) for ventricular measurements and a positive absolute rescan difference for atrial measurements.

4.1. Clinical implication and future directions

Approximately 20 million chest CT scans are performed annually in the United States and routinely archived in Picture Archiving and Communication Systems (PACS) [1]. Although many of these scans were originally acquired for non-cardiac indications, they can be repurposed for cardiac chamber volumetry and cardiovascular risk assessment, offering earlier opportunities for prevention of cardiovascular disease in those found to be at increased risk [1]. However, the majority of archived CT scans are non-gated, which has historically limited their use for cardiac analysis [7]. Our findings suggest that also (non-gated) chest CT scans can provide important prognostic information based on chamber size, with comparable performance to ECG-gated scans in predicting HF and AF. This finding can expand the pool of usable imaging data by nearly 20-fold [7], providing a vast, readily available, and cost-free resource. Leveraging these existing scans could therefore substantially reduce healthcare costs by minimizing the need for additional dedicated cardiac imaging.

Traditional risk factor based estimating the risk of AF and HF remains underutilized [35–37]. According to the AHA and the Heart Rhythm Society, it has not been established that patients identified as high risk for AF by validated risk scores actually benefit from screening or interventions aimed at reducing ischemic stroke, systemic embolism, or mortality [35]. Similarly, for HF, the clinical utility of blood biomarkers and traditional risk prediction models remains uncertain and limited [36,37]. In this context, opportunistic, AI-derived measurement of cardiac chamber size from non-gated NCCT scans, often obtained for other indications such as trauma or lung cancer screening, may help bridge this gap by alerting physicians to elevated risk, complementary to guideline-recommended risk factors. Importantly, when such assessment is based on data already acquired from routine non-gated NCCT scans, it can overcome common barriers associated with echocardiography, cardiac MRI, or ECG-gated NCCT, such as the need for specialized operators, high out-of-pocket costs, and concerns about incidental findings.

However, a key challenge in applying cardiac chamber volumetry derived from non-gated NCCT scans lies in the need for robust reference limits that define normal values. As with all imaging-based assessments, accurate interpretation depends on the availability of well-established normative data [22]. Therefore, large cohorts of healthy individuals across a wide range of ages are needed to establish reference ranges for all cardiac chamber sizes, accounting for both age and sex differences based on non-gated CT measurements. Meanwhile, similar to echocardiography, a percentile-based risk assessment offers a practical way of implementing our discoveries into routine patient care. For example, asymptomatic patients in the top 2.5th percentile of LA or LV could be flagged for further investigations [22,23]. Although this approach may be effective for population-level screening, its application at the individual patient level remains challenging, as atrial and ventricular volumes vary across different phases of the cardiac cycle. As a practical strategy, the use of chamber size ratios (e.g., LV/RV) may provide more phase-independent metrics. Alternatively, more advanced solutions, such as CT systems with higher temporal resolution that enable acquisition of multiple cardiac phases within a single scan, or the development of intrinsic gating techniques [38], may further improve accuracy in future applications.

4.2. Limitations

The MESA study has several limitations related to outcome definitions. For instance, the diagnosis of HF was limited to symptomatic individuals, which may have led to underdiagnosis by excluding asymptomatic cases. Similarly, AF may have been under detected due to the presence of paroxysmal subtypes that are difficult to identify without continuous monitoring tools such as ECG rhythm monitors or wearable devices, methods that are not feasible in large, population-based cohorts. Another limitation is the potential impact of differing ECG-gating techniques (R–R interval settings) used in MESA Exam 1, where both multidetector CT (MDCT) and electron-beam CT (EBCT) scanners were employed. However, in Exam 5, all scans were performed using MDCT, ensuring greater consistency in image acquisition. This difference in scanner technology resulted in significant variation in LA volume measurements, with lower values observed in EBCT compared to MDCT scans (57.4 mL vs. 65.4 mL, $p < 0.0001$). In contrast, LV volume and LV mass measurements remained clinically consistent across scanner types (**Table S3**). Cox models were adjusted for age and sex only; full multivariable adjustment was not performed because bootstrap-based confidence interval estimation for C-index differences becomes unstable with increasing model complexity in datasets of this size. Lastly, this analysis was conducted on a population with a mean age of approximately 70 years. Therefore, larger cohorts of healthy individuals spanning a broader age range are specifically needed to establish accurate reference ranges for all cardiac chamber sizes.

5. Conclusion

AI-derived cardiac chamber measurements obtained from ECG-gated and non-gated NCCT scans can demonstrate comparable predictive performance for HF and AF, underscoring the potential of automated AI-based volumetry across different acquisition settings. These findings suggest that non-gated chest CT scans, already performed in tens of millions of patients annually for non-cardiac indications, may represent an untapped resource for large-scale, opportunistic cardiovascular screening. This approach can expand the reach of preventive cardiology,

offering a scalable, cost-effective pathway to identify and manage cardiovascular disease earlier, especially in populations who otherwise lack access to dedicated cardiac imaging.

Abbreviations	
AF	Atrial Fibrillation
AI	Artificial Intelligence
AHA	American Heart Association
BSA	Body Surface Area
BMI	Body Mass Index
CAC	Coronary Artery Calcium
CVD	Cardiovascular Disease
CT	Computed Tomography
COPD	Chronic Obstructive Pulmonary Disease
EBCT	Electron-Beam Computed Tomography
ECG	Electrocardiogram
FDA	U.S. Food and Drug Administration
HDL-C	High-Density Lipoprotein Cholesterol
HF	Heart Failure
ICC	Intraclass Correlation Coefficient
ICD	International Classification of Diseases
LA	Left Atrium / Left Atrial
LAVI	Left Atrial Volume Index
LDL-C	Low-Density Lipoprotein Cholesterol
LoA	Limits of Agreement
LV	Left Ventricle / Left Ventricular
LVMI	Left Ventricular Mass Index
LVVI	Left Ventricular Volume Index
MDCT	Multidetector Computed Tomography
MESA	Multi-Ethnic Study of Atherosclerosis
MRI	Magnetic Resonance Imaging
NCCT	Non-Contrast Chest Computed Tomography
PACS	Picture Archiving and Communication System
RV	Right Ventricle / Right Ventricular
SD	Standard Deviation
LoA	Limits of Agreement
κ (Kappa)	Cohen's Kappa Statistic

Funding disclosures

MESA was supported by contracts 75N92025D00022, 75N92020D00001, HHSN268201500003I, N01-HC-95159, 75N92025D00026, 75N92020D00005, N01-HC-95160, 75N92020D00002, N01-HC-95161, 75N92025D00024, 75N92020D00003, N01-HC-95162, 75N92025D00027, 75N92020D00006, N01-HC-95163, 75N92025D00025, 75N92020D00004, N01-HC-95164, 75N92025D00028, 75N92020D00007, N01-HC-95165, N01-HC-95166, N01-HC-95167, N01-HC-95168 and N01-HC-95169 from the National Heart, Lung, and Blood Institute, and by grants UL1-TR-000040, UL1-TR-001079, and UL1-TR-001420 from the National Center for Advancing Translational Sciences (NCATS). Preparation of the manuscript was also supported by funding from HeartLung.AI. HeartLung Corporation is self-funded and NIH-SBIR funded. HeartLung SBIR funding number 1R43HL174376-01.

Authors contribution

M.N involved in the design and concept of the study. S.R.M prepared the primary draft and interpreted the results. K.A, A.P.R, C.Z and J.W involved in data analysis. A.A, A.H, M.M, AG, T.A, C.I. H, D.F.Y, J.J.Z, J I.M, A.B, WF, R.V, K.N, Z.F, M.V. M., J.S.R, R.V, D.J.M, J.N, K.W, P.K.S, M.J.B, D.L, R.M, OM, AA, R.A.K, N.D.W. reviewed and edited the manuscript critically. All authors edited, reviewed, and approved the final version of the manuscript. M.N is the guarantor of this work and, as such, had full access to all the data in the study and takes responsibility for the integrity of the data and the accuracy of the data analysis.

CRediT authorship contribution statement

Seyed Reza Mirjalili: Writing – review & editing, Writing – original draft, Conceptualization. **Kyle Atlas:** Writing – review & editing. **Anthony P. Reeves:** Writing – review & editing. **Chenyu Zhang:** Writing – review & editing. **Jakob Wasserthal:** Writing – review & editing. **Amir Azimi:** Writing – review & editing, Writing – original draft. **Ali Hashemi:** Writing – review & editing. **Mohammadhossein Mozafarybazargany:** Writing – review & editing. **Amir Ghaffari Jolfayi:** Writing – review & editing. **Thomas Atlas:** Writing – review & editing. **Claudia I. Henschke:** Writing – review & editing. **David F. Yankelevitz:** Writing – review & editing. **Javier J. Zulueta:** Writing – review & editing. **Wenjun Fan:** Writing – review & editing. **Jeffrey I. Mechanick:** Writing – review & editing. **Andrea D. Branch:** Writing – review & editing. **Khurram Nasir:** Writing – review & editing. **Zahi Fayad:** Writing – review & editing. **Michael V. McConnell:** Writing – review & editing. **Jamal S. Rana:** Writing – review & editing. **Rozemarijn Vliegenthart:** Writing – review & editing. **David J. Maron:** Writing – review & editing. **Jagat Narula:** Writing – review & editing. **Matthew J. Budoff:** Writing – review & editing. **Roxana Mehran:** Writing – review & editing. **Kim A. Williams Sr:** Writing – review & editing. **Prediman K. Shah:** Writing – review & editing. **Oren Mechanic:** Writing – review & editing. **Arthur S Agatston:** Writing – review & editing. **Robert A. Kloner:** Writing – review & editing. **Nathan D. Wong:** Writing – review & editing. **Morteza Naghavi:** Writing – review & editing, Conceptualization.

Declaration of competing interest

Several members of the writing group are inventors of the AI tool mentioned in this paper. M.N. is the founder of HeartLung.AI. A.P.R., T. A., D.F.Y., N.D.W., and D.L. are advisors to HeartLung.AI. C.Z. is a software engineer for HeartLung.AI. K.A. is a graduate research associate of HeartLung.AI. S.RM, and A.A, A.H, and MM are research fellows for HeartLung.AI. M.V.M is Chief Health Officer for Toku, Inc. and advisor for Porter Health. D.J.M. reports research funding from Cleerly, Inc. and consultant fees from Heartflow. The remaining authors declare no competing interests.

Supplementary materials

Supplementary material associated with this article can be found, in the online version, at doi:10.1016/j.ajpc.2026.101732.

Data availability

MESA data are available upon approval of a manuscript proposal and completion of a Data and Materials Transfer agreement.

References

[1] Smith-Bindman R, Chu PW, Azman Firdaus H, et al. Projected lifetime cancer risks from current computed tomography imaging. JAMA Intern Med 2025;185:710.
[2] Christensen JD, Harowicz M, Walker CM, et al. ACR appropriateness Criteria® chronic dyspnea-noncardiovascular origin: 2024 update. J Am Coll Radiol 2025; 22:S163–76.
[3] Kasuga I, Maezawa H, Gamo S, et al. Evaluation of chest radiography and low-dose computed tomography as valuable screening tools for thoracic diseases. Medicine 2022;101:e29261.
[4] TQIP A. Best pract guidel imaging2022.
[5] Wheeler JH, Fishman EK. Computed tomography in the management of chest infections: current status. Clin Infect Dis 1996;23:232–40.
[6] Raju S, Ghosh S, Mehta AC. Chest CT signs in pulmonary disease: a pictorial review. Chest 2017;151:1356–74.
[7] Shin JM, Kim TH, Kim JY, Park CH. Coronary artery calcium scoring on non-gated, non-contrast chest computed tomography (CT) using wide-detector, high-pitch and fast gantry rotation: comparison with dedicated calcium scoring CT. J Thorac Dis 2020;12:5783–93.
[8] Naghavi M, Reeves AP, Atlas K, et al. Artificial intelligence applied to coronary artery calcium scans (AI-CAC) significantly improves cardiovascular events prediction. npj Digit Med 2024;7:309.
[9] Naghavi M, Atlas K, Reeves AP, et al. AI-enabled opportunistic left ventricular volumetry in coronary artery calcium scans predicts heart failure comparably to cardiac MRI: an AI-CVD study with the multi-ethnic study of atherosclerosis (MESA). J Cardiovasc Comput Tomogr 2025.

[10] Naghavi M, Reeves Anthony P, Atlas Kyle C, et al. AI-enabled CT cardiac chamber volumetry predicts atrial fibrillation and stroke comparable to MRI. JACC: Adv 2024;3:101300.
[11] Naghavi M, Mirjalili R, Atlas K, et al. AI-enabled cardiac chambers volumetry interactions with diabetes for incident heart failure: an AI-CVD study. J Cardiovasc Comput Tomogr 2025;19:S52.
[12] Mirjalili SR, Atlas K, Reeves AP, et al. AI-derived left-to-right cardiac chamber volume ratios in coronary artery calcium scans strongly predict heart failure: an AI-CVD study within the multi-ethnic Study of atherosclerosis and Framingham offspring cohort. Eur Heart J - Cardiovasc Imaging 2026.
[13] Foraker R, Sperling L, Bratzke L, et al. Opportunistic detection of coronary artery calcium on noncardiac chest computed tomography: an emerging tool for cardiovascular disease prevention: a scientific statement from the American heart association. Circulation 2025.
[14] Hofmann LK, Zou KH, Costello P, Schoepf UJ. Electrocardiographically gated 16-section CT of the thorax: cardiac motion suppression. Radiology 2004;233:927–33.
[15] Kerkhof PLM, Kuznetsova T, Yasha Kresh J, Handly N. Cardiophysiology illustrated by comparing ventricular volumes in healthy adult males and females. Adv Exp Med Biol 2018;1065:123–38.
[16] Detrano RC, Anderson M, Nelson J, et al. Coronary calcium measurements: effect of CT scanner type and calcium measure on rescan reproducibility—MESA study. Radiology 2005;236:477–84.
[17] Kim JS, Kim J, Yin X, et al. Associations of hiatus hernia with CT-based interstitial lung changes: the MESA Lung Study. Eur Respir J 2023:61.
[18] Eng D, Chute C, Khandwala N, et al. Automated coronary calcium scoring using deep learning with multicenter external validation. npj Digit Med 2021;4:88.
[19] Carr JJ, Nelson JC, Wong ND, et al. Calcified coronary artery plaque measurement with cardiac CT in population-based studies: standardized protocol of multi-ethnic study of atherosclerosis (MESA) and coronary artery risk development in young adults (CARDIA) study. Radiology 2005;234:35–43.
[20] Horwich T, Srikanthan P, Gaitonde A, Watson K, Allison M, Kronmal R. Association between measures of body composition and coronary calcium: findings from the multi-ethnic study of atherosclerosis. J Am Heart Assoc 2023;12:e027708.
[21] Ichikawa K, Wang R, McClelland RL, et al. Thoracic versus coronary calcification for atherosclerotic cardiovascular disease events prediction. Heart 2024;110:947–53.
[22] Kou S, Caballero L, Dulgheru R, et al. Echocardiographic reference ranges for normal cardiac chamber size: results from the NORRE study. Eur Heart J Cardiovasc Imaging 2014;15:680–90.
[23] Lang RM, Badano LP, Mor-Avi V, et al. Recommendations for cardiac chamber quantification by echocardiography in adults: an update from the American society of echocardiography and the european association of cardiovascular imaging. J Am Soc Echocardiogr 2015;28:1–39.e14.
[24] Bland JM, Altman DG. Measuring agreement in method comparison studies. Stat Methods Med Res 1999;8:135–60.
[25] Osborne-Grinter M, Ali A, Williams MC. Prevalence and clinical implications of coronary artery calcium scoring on non-gated thoracic computed tomography: a systematic review and meta-analysis. Eur Radiol 2024;34:4459–74.
[26] Vural M, Dölek BA, Kılıçkap G, Kübra Bahadır G, Celal Güneş Y. Epicardial adipose tissue (EAT) thickness on non-gated chest CT as an alternative to EAT volume on cardiac CT. Acta Radiol 2024;65:601–8.
[27] Mineo E, Assuncao-Jr AN, Grego da Silva CF, et al. Automated coronary artery calcium scoring using deep learning: validation across diverse chest CT protocols. Acad Radiol 2025;32:7177–86.
[28] Aldana-Bitar J, Fazlalizadeh H, Kinninger A, et al. Comparison of AI derived gated versus non-gated coronary artery calcium score by vessel. J Cardiovasc Comput Tomogr 2023;17:S57.
[29] Eng D, Chute C, Khandwala N, et al. Automated coronary calcium scoring using deep learning with multicenter external validation. NPJ Digit Med 2021;4:88.
[30] Lu MT, Cai T, Ersoy H, et al. Comparison of ECG-gated versus non-gated CT ventricular measurements in thirty patients with acute pulmonary embolism. Int J Cardiovasc Imaging 2009;25:101–7.
[31] Ramanathan R, Anumandla AK, Haramati LB, et al. Evaluation of the cardiac chambers on axial CT: comparison with echocardiography. J Comput Assist Tomogr 2014;38:53–60.
[32] Shahzad R, Bos D, Budde RP, et al. Automatic segmentation and quantification of the cardiac structures from non-contrast-enhanced cardiac CT scans. Phys Med Biol 2017;62:3798–813.
[33] Abbara S, Blanke P, Maroules CD, et al. SCCT guidelines for the performance and acquisition of coronary computed tomographic angiography: a report of the society of cardiovascular computed tomography guidelines committee: endorsed by the North American society for cardiovascular imaging (NASCI). J Cardiovasc Comput Tomogr 2016;10:435–49.
[34] Walker JR, Abadi S, Solomonica A, et al. Left-sided cardiac chamber evaluation using single-phase mid-diastolic coronary computed tomography angiography: derivation of normal values and comparison with conventional end-diastolic and end-systolic phases. Eur Radiol 2016;26:3626–34.
[35] Joglar JA, Chung MK, Armbruster AL, et al. 2023 ACC/AHA/ACCP/HRS guideline for the diagnosis and management of atrial fibrillation: a report of the American college of cardiology/American heart association joint committee on clinical practice guidelines. Circulation 2024;149:e1–156.
[36] Khan SS, Berwanger O, Fiuzat M, et al. Prioritising the primary prevention of heart failure. Lancet 2025;406:1138–53.
[37] Nadarajah R, Younsi T, Romer E, et al. Prediction models for heart failure in the community: a systematic review and meta-analysis. Eur J Heart Fail 2023;25:1724–38.
[38] Dinkel J, Bartling SH, Kuntz J, et al. Intrinsic gating for small-animal computed tomography. Cardiovasc Imaging 2008;1:235–43.